



# Potential subglacial lake locations and meltwater drainage pathways beneath the Antarctic and Greenland ice sheets

S. J. Livingstone<sup>1</sup>, C. D. Clark<sup>1</sup>, J. Woodward<sup>2</sup>, and J. Kingslake<sup>3</sup>

<sup>1</sup>Department of Geography, University of Sheffield, Sheffield, S10 2TN, UK

<sup>2</sup>Department of Geography, Engineering and Environment, Northumbria University, Newcastle-Upon-Tyne, NE1 8ST, UK

<sup>3</sup>British Antarctic Survey, Madingley Road, Cambridge, UK

Correspondence to: S. J. Livingstone (s.j.livingstone@sheffield.ac.uk)

Received: 5 March 2013 – Published in The Cryosphere Discuss.: 21 March 2013

Revised: 7 October 2013 – Accepted: 15 October 2013 – Published: 11 November 2013

**Abstract.** We use the Shreve hydraulic potential equation as a simplified approach to investigate potential subglacial lake locations and meltwater drainage pathways beneath the Antarctic and Greenland ice sheets. We validate the method by demonstrating its ability to recall the locations of > 60 % of the known subglacial lakes beneath the Antarctic Ice Sheet. This is despite uncertainty in the ice-sheet bed elevation and our simplified modelling approach. However, we predict many more lakes than are observed. Hence we suggest that thousands of subglacial lakes remain to be found. Applying our technique to the Greenland Ice Sheet, where very few subglacial lakes have so far been observed, recalls 1607 potential lake locations, covering 1.2 % of the bed. Our results will therefore provide suitable targets for geophysical surveys aimed at identifying lakes beneath Greenland. We also apply the technique to modelled past ice-sheet configurations and find that during deglaciation both ice sheets likely had more subglacial lakes at their beds. These lakes, inherited from past ice-sheet configurations, would not form under current surface conditions, but are able to persist, suggesting a retreating ice-sheet will have many more subglacial lakes than advancing ones. We also investigate subglacial drainage pathways of the present-day and former Greenland and Antarctic ice sheets. Key sectors of the ice sheets, such as the Siple Coast (Antarctica) and NE Greenland Ice Stream system, are suggested to have been susceptible to subglacial drainage switching. We discuss how our results impact our understanding of meltwater drainage, basal lubrication and ice-stream formation.

## 1 Introduction

Understanding the drainage of meltwater beneath ice is fundamental to resolving ice-flow dynamics because water pressure influences both the strength of the subglacial sediment and the frictional interaction between ice and its sole (Clarke, 2005; Schoof, 2010). However, subglacial meltwater drainage is dynamic in space and time and varies in a complicated manner coupled to ice mechanics (e.g. Fountain and Walder, 1998; Nienow et al., 1998; Bartholomew et al., 2010; Kingslake and Ng, 2013). Possible meltwater networks at the ice–bed interface are thought to include (i) discrete tunnel systems (e.g. Röthlisberger, 1972; Walder and Hallet, 1979; Nienow et al., 1998); (ii) distributed networks of passages and cavities (e.g. Lliboutry, 1979; Kamb, 1987; Sharp et al., 1989); (iii) thin water films (e.g. Hallet, 1979; Lappégard et al., 2006); and (iv) Darcian flow through sediments (e.g. Hubbard et al., 1995). These drainage configurations evolve on daily to millennial timescales as basal conditions are perturbed (Hubbard et al., 1995; Bartholomew et al., 2010).

The identification of subglacial lakes beneath the Antarctic Ice Sheet (AIS) (Robin et al., 1970) has altered our perception of how meltwater drains and is stored beneath large ice masses (e.g. Smith et al., 2009). Indeed, subglacial lakes beneath the AIS are now known to comprise a crucial component of the subglacial environment, capable of actively interacting with the surrounding hydrological network and transmitting large volumes of meltwater between lakes and towards the grounding line (e.g. Wingham et al., 2006; Fricker et al., 2007; Smith et al., 2009). An inventory of over 380

known subglacial lakes has been compiled recently for the AIS (Wright and Siegert, 2012), and thus, unlike the subglacial hydrological system as a whole (i.e. the pathways and networks), we have a decent (and rapidly improving) understanding of the spatial distribution and geometry of subglacial lakes. They are therefore a valuable resource for constraining and testing glacial models (Pattyn, 2010).

Despite theoretical advances in how we understand subglacial hydrology, relatively little is known about the distribution of subglacial water and the form of the drainage system. And although subglacial lakes are being identified beneath the AIS, they have only been posited under other (palaeo-)ice sheets (e.g. Livingstone et al., 2012, 2013). One method of investigating the subglacial hydrological network is to calculate the hydraulic potential from the bed and ice-surface topographies (Shreve, 1972), and then to use simple routing techniques to derive first-order approximations of meltwater flow paths and subglacial lakes (e.g. Evatt et al., 2006; Siegert et al., 2007; Wright et al., 2008). This method has potential application in predicting and investigating subglacial hydrological systems in both contemporary and palaeo-settings, and it is therefore important to verify how well it can reproduce known subglacial drainage configurations.

In this paper, potential subglacial lake locations and meltwater drainage pathways are calculated both for the present-day Antarctic and Greenland ice sheets, and over the last 20 000 yrs of their evolution. The inventory of subglacial lakes for the AIS (Wright and Siegert, 2012) is used to test whether the hydraulic potential can be used to recall the pattern of known present-day subglacial lakes. Because much of the ice thickness and bed topography are derived from radar data that represent the surface of subglacial lakes at the bed, the hydraulic potential surface will include a representation of the surface of known lakes. This may preclude their identification. If known subglacial lakes can be recalled our approach will allow us to locate subglacial lakes that have not been observed yet. Derived subglacial meltwater flow paths provide information on hydrological connections, the structure of the drainage system and their association with ice streams (see Siegert et al., 2007). Subglacial meltwater pathways and lakes calculated at time slices through the past deglaciation, of the Antarctic and Greenland ice sheets, using the output of independent models (not coupled to our simple hydrological model) allow an assessment of the sensitivity of subglacial hydrological pathways and subglacial lakes to large-scale ice-sheet evolution (e.g. Wright et al., 2008).

## 2 Methods

### 2.1 Calculating subglacial water flow and storage

The flow and storage of meltwater under ice masses is principally governed by gradients in the hydraulic potential ( $\Phi$ ),

which is a function of the elevation potential and water pressure (Shreve, 1972):

$$\Phi = \rho_w gh + P_w, \quad (1)$$

where  $\rho_w$  is the density of water ( $1000 \text{ kg m}^{-3}$ ),  $g$  is the acceleration due to gravity,  $h$  is the bed elevation and  $P_w$  is the water pressure. The subglacial water pressure can be expressed as a function of the ice overburden pressure and effective pressure,  $N$ :

$$P_w = \rho_i g H - N, \quad (2)$$

where  $\rho_i$  is the density of ice ( $917 \text{ kg m}^{-3}$ ) and  $H$  is the ice thickness. Subglacial water pressures vary in a complex way due to temporally and spatially varying drainage-pathway capacities and the filling and drainage of lakes. However, limited borehole observations suggest that  $P_w$  is close to the ice overburden pressure (e.g. Kamb, 2001). As our aim is to estimate the average, large-scale behaviour of drainage systems we can therefore assume that  $N=0$ , allowing us to re-write Eq. (1) as

$$\Phi = \rho_w gh + \rho_i g H, \quad (3)$$

We evaluate  $\Phi$  in a GIS using the Shreve equation and gridded data pertaining to  $h$  and  $H$ . This produces a hydraulic potential surface over which water is routed using a routing algorithm from the ArcHydro package (part of the GIS software ArcMap) to estimate the large-scale structure of the subglacial drainage systems of the Greenland and Antarctic ice sheets. At each GIS grid cell the algorithm calculates the hydraulic potential gradient in each direction, then routes water in the direction of the largest hydraulic gradient. Drainage pathways are calculated by defining the cumulative number of all cells that flow into each downslope cell. Output cells with a high flow accumulation represent concentrated subglacial meltwater flow and are therefore potential subglacial meltwater pathways (see also Siegert et al., 2007; Wright et al., 2008). Another algorithm in the ArcHydro package was used to identify minima in the hydraulic potential surface. Following previous authors (e.g. Evatt et al., 2006; Livingstone et al., 2013), we associate these minima with likely locations of subglacial lakes by filling them to their lip.

Equation (3) can be re-arranged to demonstrate the well-known result that the contribution of the ice-surface gradient to the hydraulic potential is a factor of  $\approx 10$  times that of the bed gradient. Thus, the ice surface, which is capable of rapid changes in elevation and slope, is the primary driver of subglacial water. However, the weaker influence of the bed is partially offset by its greater relief and spatial variability (Wright et al., 2008).

Using the Shreve equation to derive first-order potential subglacial lake locations and meltwater drainage pathways is simple and quick to implement but has a number of limitations. Crucially the subglacial meltwater and overlying ice

**Table 1.** Recall and precision of potential present-day AIS subglacial lake locations: all the potential lakes were calculated using a 1 km grid resolution, with a threshold size of 5 km<sup>2</sup> used to identify hydraulic sinks (subglacial lakes). The known lakes are derived from Wright and Siegert (2012); <sup>a</sup>warm-bedded refers to the inclusion of modelled basal temperature (Pattyn, 2010); and the modelled 0 ka time slice is from Whitehouse et al. (2012)

Subglacial lake predictions		Standard	Smoothed (focal mean)	Modelled 0 ka time slice
Frequency	BEDMAP2	12767	4536	5232
	Warm-bedded <sup>a</sup>	9360	–	–
Recall (percentage)	BEDMAP2	61	36	38
	Known lakes $\geq$ 5 km	79	68	69
	Warm-bedded <sup>a</sup>	60	–	–
	Warm-bedded and with known lakes $\geq$ 5 km	64	–	–
Precision (percentage)	BEDMAP2	3.7	4.3	3.9
	Warm-bedded <sup>a</sup>	3.9	–	–

are not dynamically coupled, so we have to assume a uniform (zero)  $N$  and a warm-basal thermal regime. In particular, our simple approach is not likely to be valid at small (metre) scales where local processes dominate  $N$ , although when averaged over larger (kilometre) scales the main control on subglacial drainage is likely to be ice-sheet geometry. However, as subglacial lakes can originate entirely from coupled ice-dynamic–meltwater processes, some lakes will not be identified using this approach. This includes those formed in the lee of high basal traction areas such as bedrock bumps or “sticky spots” (Fricker et al., 2010; Sergienko and Hulbe, 2011), by high geothermal heat fluxes or behind frozen margins (see Livingstone et al., 2012). Finally, because the ice surface, lakes and drainage pathways are treated independently the use of modelled output to investigate palaeo-subglacial lakes cannot include coupled processes such as the ice-surface flattening feedback effect that will modify the evolution of both the drainage network and ice-sheet geometry over time.

## 2.2 Antarctic datasets and statistics

Ice-surface and bed topographies were taken from BEDMAP2, which is interpolated from 25 million measurements of ice thickness and constructed at 1 km resolution (Fretwell et al., 2013). The formation of subglacial lakes influences ice dynamics and causes a flattening of the ice-surface slope. This opens up a potentially circular argument because the calculations will tend to pick up the resultant flat ice surfaces rather than the initial hydraulic minima that caused the subglacial lake to form. To account for this circularity the ice surface of BEDMAP2 was also smoothed to remove surface features using a focal mean with a 10 and 20 km circular window. However, as the smoothing algorithm can more easily remove smaller ice-surface features,

the effect will be biased by subglacial lake size. To account for this we also used a modelled present-day ice surface (see Whitehouse et al., 2012, for a full description of the model) derived from the Glimmer community ice-sheet model (Rutt et al., 2009). The model produces very smooth ice surfaces and can therefore be used as a comparative smoothing experiment to check for any bias in the aforementioned smoothing algorithm. Deglacial ice and bed topographies at 5, 10, 15 and 20 thousand year intervals were also derived from the Glimmer community ice-sheet model (Rutt et al., 2009). The ice-surface output was resampled to 1 km resolution and the bed topography output was used to correct the present-day BEDMAP2 digital elevation model (DEM) for isostasy. These were then used to calculate the hydraulic potential from the Shreve equation (Eq. 3). In addition to the caveats discussed in Section 2.1, this approach is likely to accrue error because we are up-scaling the ice-surface and bed topographies used in the model, while the lack of surface structure precludes a direct comparison with the present-day predictions. Nevertheless, it does allow a relative comparison of potential subglacial lake locations and their evolution during deglaciation. Importantly, the ice margins and thicknesses are constrained by an extensive database of geological and glaciological information (see Whitehouse et al., 2012).

To assess the accuracy of the Shreve equation in identifying potential subglacial lake locations we validated our results against the latest subglacial lake inventory (Wright and Siegert, 2012). Although the bed grids are interpolated at 1 km resolution (Fretwell et al., 2013), the smallest features that it resolves are 5 km<sup>2</sup>. Therefore, we use 5 km<sup>2</sup> as the threshold lake area. In comparison, the smallest known subglacial lake has a length of 478 m, while the majority of those identified are < 10 km long (Wright and Siegert, 2012). A simulated subglacial lake was deemed successful in

identifying a known subglacial lake if it was within a buffer defined by the known lake's length (true positive). Where the subglacial lake's length was not recorded or known we used the modal length (5 km), taken from the recent lake inventory (Wright and Siegert, 2012). Two statistics were calculated to characterise the ability of the simulations to replicate the known distribution of subglacial lakes, where false negatives are known subglacial lakes that the model cannot predict and false positives are subglacial lakes which are simulated that do not conform to known subglacial lake locations:

- Recall (the percentage of known subglacial lakes identified by the predictions) =  $\text{true positives}/(\text{true positives} + \text{false negatives}) \times 100$ ;
- Precision (the percentage of the predictions that correspond to a known subglacial lake location) =  $\text{true positives}/(\text{true positives} + \text{false positives}) \times 100$ .

Despite the significant improvements of BEDMAP2 over its predecessors there are still large regions that suffer from insufficient input data, resulting in estimated vertical elevation uncertainties of > 100 m over 76 % of the bed (Fretwell et al., 2013). To explore the sensitivity of our potential subglacial lake locations to uncertainty in the bedrock elevation we carried out 50 random perturbations of the bed elevation DEM in which each grid point was randomly perturbed using a normal distribution with a standard deviation equal to the uncertainty in the bed elevation. The sensitivity of the potential subglacial lake locations was also investigated by calculating the recall and precision of known subglacial lakes  $\geq 5$  km long to see whether lake size has any influence on predictability. Finally, although we assume a warm-basal thermal regime when calculating the Shreve equation, ice sheets are in fact polythermal and so basal melting will vary across the bed. Crucially, when the ice temperature falls below the pressure melting point (cold bedded) basal melting will be absent. Basal ice temperature therefore influences the potential for lake formation and the drainage of meltwater. To try to account for this effect we performed an additional experiment using a modelled basal thermal regime (from Pattyn, 2010) to mask out subglacial lakes and drainage pathways calculated to form in cold-bedded regions of the bed where meltwater is absent (Fig. 1b).

### 2.3 Greenland datasets

DEMs of ice-surface and bed topographies (from Bamber et al., 2013) were used to calculate the hydraulic potential surface of the Greenland Ice Sheet (GrIS) on a 1 km grid, from which we derived potential lake positions using the same routing algorithm as before and a 5 km<sup>2</sup> threshold. We explored the sensitivity of the potential subglacial lake locations to uncertainty in the bed elevation data by running 50 perturbation experiments using the same approach as was used for the AIS.

To investigate subglacial hydrological changes of the GrIS since the Last Glacial Maximum (LGM, 21 thousand years ago), output from Huy2, a three-dimensional thermomechanical model (Simpson et al., 2009), was used to produce ice-surface and bed topographies at 1 thousand year time slices through the evolution of the ice sheet. For this exercise the Bamber et al. (2001a, b) 5 km grid was used to maintain consistency with the numerical modelling. Importantly, the model is constrained by, and in good agreement with, observations of relative sea level as well as field data on past ice extent (Simpson et al., 2009). Likelihood maps indicating the percentage time that subglacial lakes existed throughout deglaciation thus far were derived, to explore the stability and evolution of the simulated subglacial lakes.

## 3 Simulating subglacial meltwater drainage and lakes under the Antarctic Ice Sheet

### 3.1 Present-day Antarctic Ice Sheet

The subglacial drainage pattern produced for the BEDMAP2 dataset (grid size of 1 km) is displayed in Fig. 1a, and provides an update of the work presented by Wright et al. (2008), which used BEDMAP (grid size of 5 km). Meltwater flow is arranged in a series of discrete catchments, with meltwater flowing from central ice divides towards the margin. Drainage networks reveal subtle variations in their geometry. These can be characterised as (i) classical dendritic; (ii) angular; (iii) convergent; and (iv) parallel patterns (see inset circles in Fig. 1a). Subglacial meltwater tends to be concentrated along the major ice streams where the ice surface is lower than the surrounding ice sheet. Of the known subglacial lakes, the largest, Subglacial Lake Vostok (East Antarctica), is shown to drain through the Transantarctic Mountains (Fig. 1a).

Fig. 1

When the ice surface is smoothed using the focal mean and indirectly with the modelled present-day ice surface the simulated drainage pathways remain broadly similar to the standard experiment. Subtle differences are associated with the capture of Ice Stream E (MacAyeal) by Ice Stream D (Bindshadler) by both the smoothing algorithm and modelled present-day ice surface; drainage of Subglacial Lake Vostok through Wilkes Land using the model output; and capture of the upper half of the Recovery Glacier drainage network by Slessor Glacier again using the model output. When a cold-bedded mask is applied, and the subglacial meltwater routing recalculated using just the warm-based nodes, the size of the drainage catchments are much reduced, particularly in East Antarctica where many of the meltwater pathways are cut off before they reach the grounding line (Fig. 1b). Indeed, the drainage pathways of many of the subglacial lakes become cut off when the cold-bedded mask is included (e.g. Subglacial Lake Vostok), while the source areas are in some

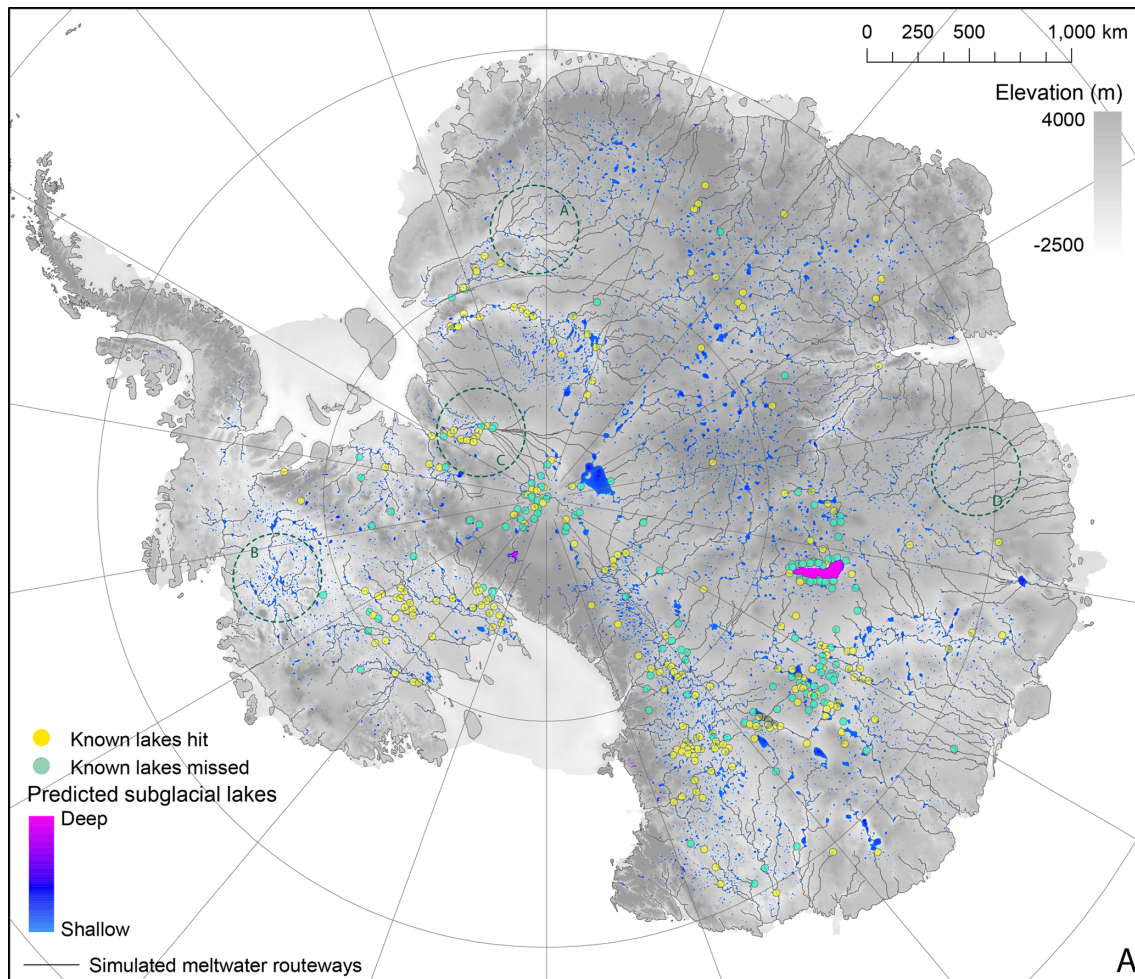


**Fig. 1.** Simulated subglacial drainage pathways and subglacial lakes beneath the AIS. (A) Warm-based thermal regime. The four dark-green dotted circles illustrate the different types of drainage pattern (after Twidale, 2004) that characterise the bed of Antarctica (A: classical dendritic; B: angulate; C: convergent; and D: parallel). The simulated drainage networks are visually defined as cells which have more than 5000 cumulative cells flowing into them.

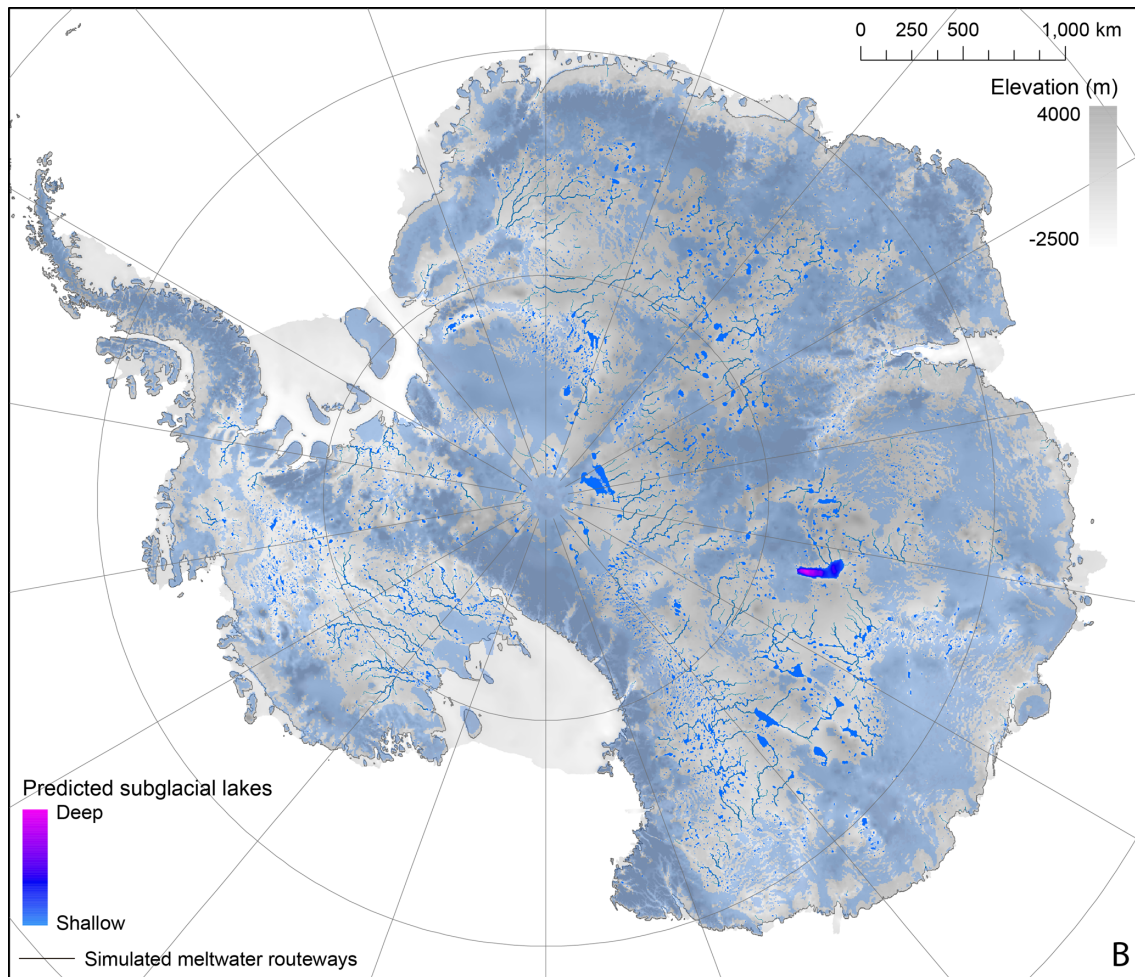
cases much reduced (e.g. subglacial lakes associated with the Recovery Glacier).

Fig. 5

Simulated subglacial lakes are relatively commonplace, with 12 767 occurring over  $\sim 4\%$  of the grounded AIS (Fig. 1a, Table 1), dropping to 9 360 and 2.7% respectively when cold-bedded regions are masked out (Fig. 1b, Table 1). They are prevalent beneath the East and West Antarctic ice sheets, occurring at a range of scales and congregating beneath ice streams and ice divides, often along or at the source of major subglacial drainage routeways. Rugged regions of the bed display a greater tendency towards ponding, as do localities where the ice-surface has a rough texture; the curvilinear distribution of simulated subglacial lakes inland of the Transantarctic Mountains is primarily a result of such rough surface structure. The largest subglacial lakes are observed beneath ice divides, with the largest located close to the

South Pole and second-largest successfully delimiting Subglacial Lake Vostok (Fig. 1a). In contrast, they are relatively rare beneath the rugged Antarctic Peninsula hinterland where they typically form small lakes.

Of the known subglacial lakes, 61% are successfully recalled using the Shreve equation, rising to 79% when just those known lakes  $\geq 5$  km long are considered (Table 1; Fig. 1a). The most successful recall of known subglacial lakes occurs along the Siple Coast, in Victoria Land and down the Academy and Recovery glaciers, with the poorest recalls associated with the cluster of lakes around Subglacial Lake Vostok, south of  $86^\circ\text{S}$  and in the Aurora and Vincennes subglacial basins (Fig. 1a). Indeed, known subglacial lakes beneath ice streams tend to be more easily recalled than those associated with ice-divide locations. The smoothed and modelled present-day ice surfaces produce similar recall rates, with a low recall ( $< 40\%$ ) when all the known subglacial



**Fig. 1. (B)** Polythermal basal thermal regime (from Pattyn, 2010). The blue colour illustrates regions below the pressure melting point. This is used as a simple mask to remove all subglacial lakes that fall within the cold-bedded zones. The simulated drainage networks are visually defined as cells which have more than 5000 cumulative cells flowing into them, with a secondary threshold of 2000 cells (finer lines).

lakes are included, rising substantially ( $> 65\%$ ) when just analysing the known lakes  $\geq 5$  km long (Table 1).

Given the high frequency of potential subglacial lake locations (Table 1) it is conceivable the high recalls could occur by chance. In other words, the large number of potential subglacial lake locations may preclude a low percentage of hits because they occupy a large expanse of the ice-sheet bed. To test this we randomly redistributed the 386 known subglacial lakes and recalculated the recall. Despite carrying out multiple iterations, significantly lower percentages (30–35%) are consistently recorded. This gives us confidence that the high recalls are real and not an artefact of chance.

For the same scenarios, we also looked at the precision of potential subglacial lake locations. This is more complicated because we do not have a complete inventory of subglacial lakes, and so a false-positive result does not preclude a correct prediction. Of the 12 767 potential subglacial lake locations predicted for the present-day ice sheet only 3.7% oc-

cur within the buffer zone of known lake localities, with this figure rising to 3.9% when subglacial lakes in cold-bedded regions of the AIS are masked out. This is comparable to the precision of both smoothing experiments (Table 1).

Figure 1c displays the sensitivity results of potential subglacial lake locations to uncertainty in the bed elevation dataset, expressed as a lake persistence (i.e. which lakes persist through a large number of random perturbations). The potential subglacial lake locations least sensitive to perturbations in the bed elevation uncertainty tend to be the largest. This is expected because the horizontal dimensions of these subglacial lakes far exceed the vertical dimensions. Significantly many lakes which occur infrequently when the bed is perturbed ( $< 50\%$  persistent) occur in regions that are characterised by limited or no data, such as Princess Elizabeth Land and between Recovery and Support Force glaciers (see Fretwell et al., 2013). Indeed, when just those subglacial lakes with a  $> 50\%$  persistence are included in the analysis

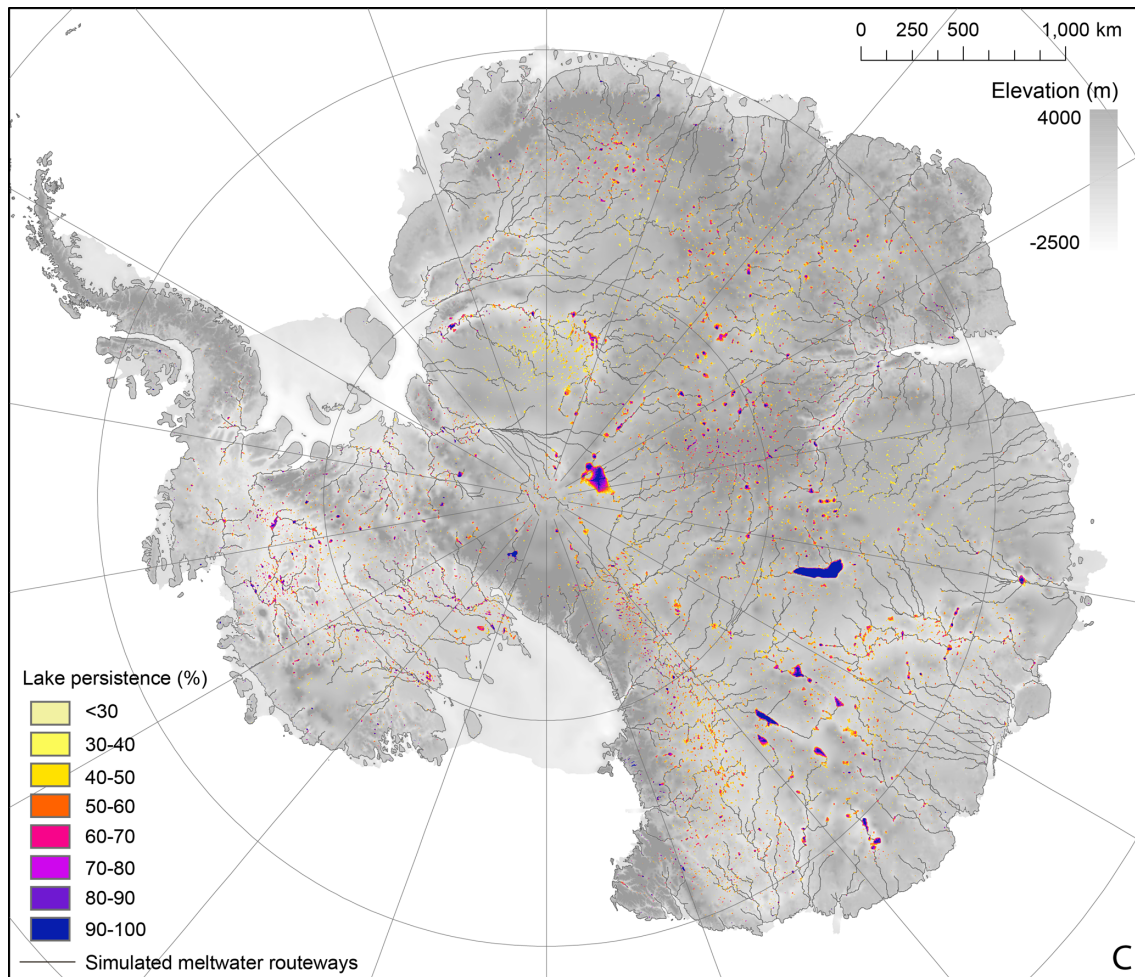


**Fig. 1. (C)** Subglacial lake persistence in response to 50 random bed elevation perturbation experiments, using a normal distribution with a standard deviation equal to the vertical bed elevation uncertainty. The simulated drainage networks are visually defined as cells which have more than 5000 cumulative cells flowing into them.

the recall remains high (58 % and 76 % with known lakes  $\geq 5$  km long), while the precision increases to 5 %. Higher lake persistence values result in a sharp fall in recall. For instance, those simulated subglacial lakes with a  $\geq 90$  % persistence recall just 16 % of the known subglacial lakes.

### 3.2 Deglaciation of the Antarctic Ice Sheet since the LGM

Figure 2 reveals the simulated drainage patterns and potential subglacial lake locations at 20, 15 and 5 thousand year time slices during the deglaciation of the AIS. These suggest that meltwater drainage under the AIS was relatively stable throughout deglaciation thus far, with drainage configurations comparable to the present-day ice sheet (see Fig. 1a). However, significant meltwater switches and drainage capture are observed. For instance, meltwater flow from Subglacial Lake Vostok, which is currently thought to drain through the Transantarctic Mountains (Fig. 1a), is simulated

to drain towards Wilkes Land during the four deglacial time slices (Fig. 2). Furthermore, the Siple Coast drainage network repeatedly shifted position as ice retreated (see Fig. 3). Indeed, at the 15 000 yr time-slice meltwater was captured and focused through a single pass in the Transantarctic Mountains, while at 20 and 10 thousand years before present two major drainage routeways were thought to have been in operation (Fig. 3). By 10 000 yr ago, the westernmost drainage network (basin 1 in Fig. 3) had been almost completely subsumed by its neighbouring catchment, and by 5000 yr before present West Antarctica was providing the majority of the meltwater instead of East Antarctica, which previously dominated.

Simulated subglacial lakes are relatively stable during deglaciation, especially beneath ice divides in East Antarctica. However, short-lived subglacial lake formation is predicted during expansion of ice to the shelf edge throughout the Antarctic Peninsula, parts of West Antarctica, across the

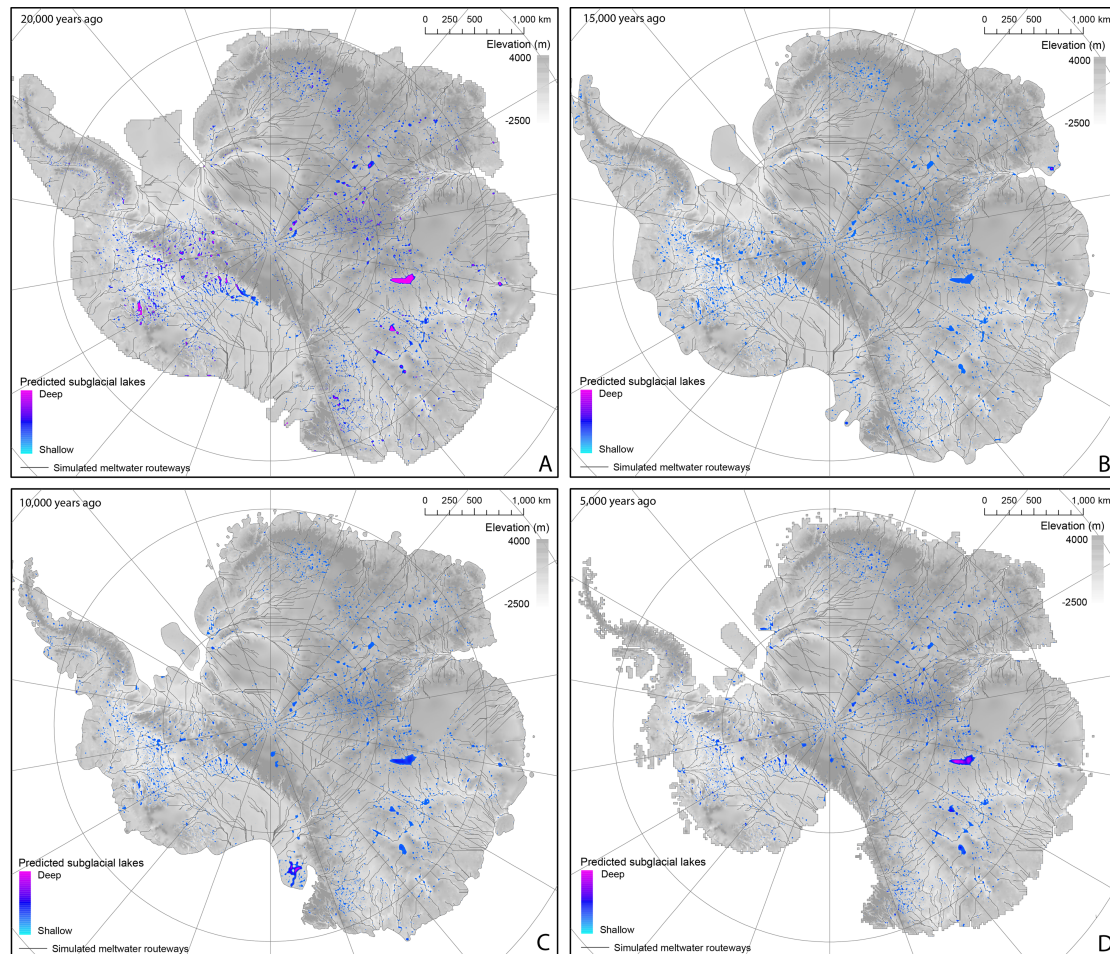


**Fig. 2.** Simulated subglacial drainage pathways and subglacial lakes at 5, 10, 15 and 20 thousand-year time slices during the deglaciation of the AIS. The ice-sheet model used is from Whitehouse et al. (2012).

continental shelf and through the Transantarctic Mountains (Fig. 2). The frequency distribution of simulated subglacial lake areas is similar for all four deglacial time slices and a similar pattern is also observed for the present-day ice-sheet configuration (Fig. 4). Although very large subglacial lakes, greater than  $300 \text{ km}^2$ , are simulated, the vast majority are  $< 10 \text{ km}^2$  in size. This pattern is comparable to the distribution of known subglacial lake lengths (Wright and Siegert, 2012).

#### 4 Simulating subglacial meltwater drainage and lakes under the Greenland Ice Sheet

Whereas subglacial lakes are commonly observed and simulated beneath the AIS (e.g. Wright and Siegert, 2012), there is almost no evidence for subglacial lakes existing beneath the GrIS (although see Ekholm et al., 1998). This seems incongruous given observations detailing the widespread presence of subglacial meltwater at its bed (Dahl-Jensen et al., 2003; Oswald and Gogineni, 2008, 2012). Is this because there are

very few subglacial lakes? If so, what conditions inhibit their formation? Or are there subglacial lakes at the bed that remain to be found?

Given the high percentage of known subglacial lakes recalled beneath the AIS (Sect. 3) we suggest that simple hydrological calculations can be a useful tool for simulating subglacial lakes and drainage pathways beneath other (palaeo-)ice sheets. With this in mind, we now investigate the subglacial drainage network of the GrIS in its present and past states, including the potential for subglacial lake formation.

##### 4.1 Present-day Greenland Ice Sheet

Subglacial lakes and meltwater drainage networks are displayed in Fig. 5, where they are compared against ice-surface velocity measurements (Joughin et al., 2010) and observed hydrological outlets at the ice-sheet margin (after Lewis and Smith, 2009).

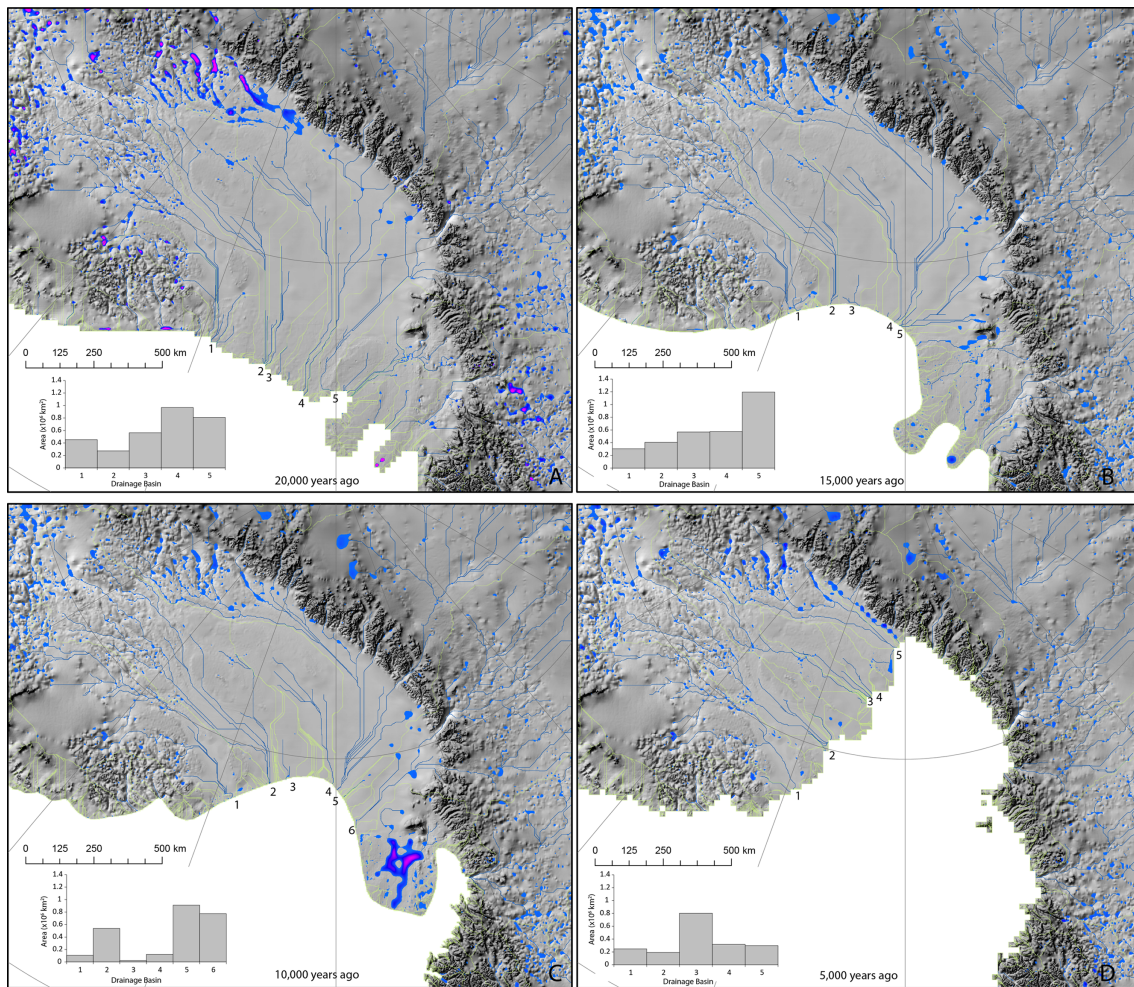


**Fig. 3.** Simulated subglacial drainage pathways and lakes at 5, 10, 15 and 20 thousand-year time slices during the deglaciation of the Siple Coast sector of the AIS. The ice-sheet model used is from Whitehouse et al. (2012). The bar charts illustrate the area of significant drainage basins and correspond to the numbering on the maps. The pale-green lines divide drainage basins.

Like Antarctica, meltwater drainage beneath the GrIS is organised into a series of discrete catchments composed of dendritic pathways that broadly flow from the ice-sheet centre to the margin (Fig. 5). Meltwater flow concentration is demonstrated along the fast-flowing corridors of the ice sheet, with significant drainage networks feeding the Northeast Greenland Ice Stream (NEGIS) ( $108\,925\text{ km}^2$ ), Jakobshavn Isbrae ( $103\,575\text{ km}^2$ ) and the Petermann Glacier ( $61\,850\text{ km}^2$ ) (Fig. 5b). A qualitative relationship is also observed between ice-surface velocity and the size of the meltwater drainage network. Moreover, a good general agreement between predicted and known meltwater outlets was demonstrated by Lewis and Smith (2009) (Fig. 5a).

The Shreve equation simulates 1 607 subglacial lakes beneath the GrIS, which cover  $\sim 1.2\%$  of the GrIS bed. The majority of lakes, particularly the larger ones, tend to occur in the rugged eastern sector of the ice sheet, although they are also prevalent along the NEGIS, Jakobshavn Isbrae

and Helheim catchments and beneath the main north–south ice divide (Fig. 5). The overall distribution of potential subglacial lake locations displays a striking similarity to the AIS (Fig. 4), although very large subglacial lakes are not produced.

The results of the bed perturbation experiments are displayed in Fig. 5c. As with Antarctica, many of the subglacial lakes that are simulated in regions characterised by little or no data are infrequent features (e.g. NW of Kangerdlugssuaq). Likewise, the largest potential subglacial lake location, in the eastern sector of the ice sheet, responds sensitively to uncertainty in the bed elevation. However, the rugged eastern sector of the ice sheet, including the NEGIS, is primarily characterised by persistent subglacial lake formation. This is also evident for the congregation of subglacial lakes associated with Jakobshavn Isbrae, which persist despite their small size.

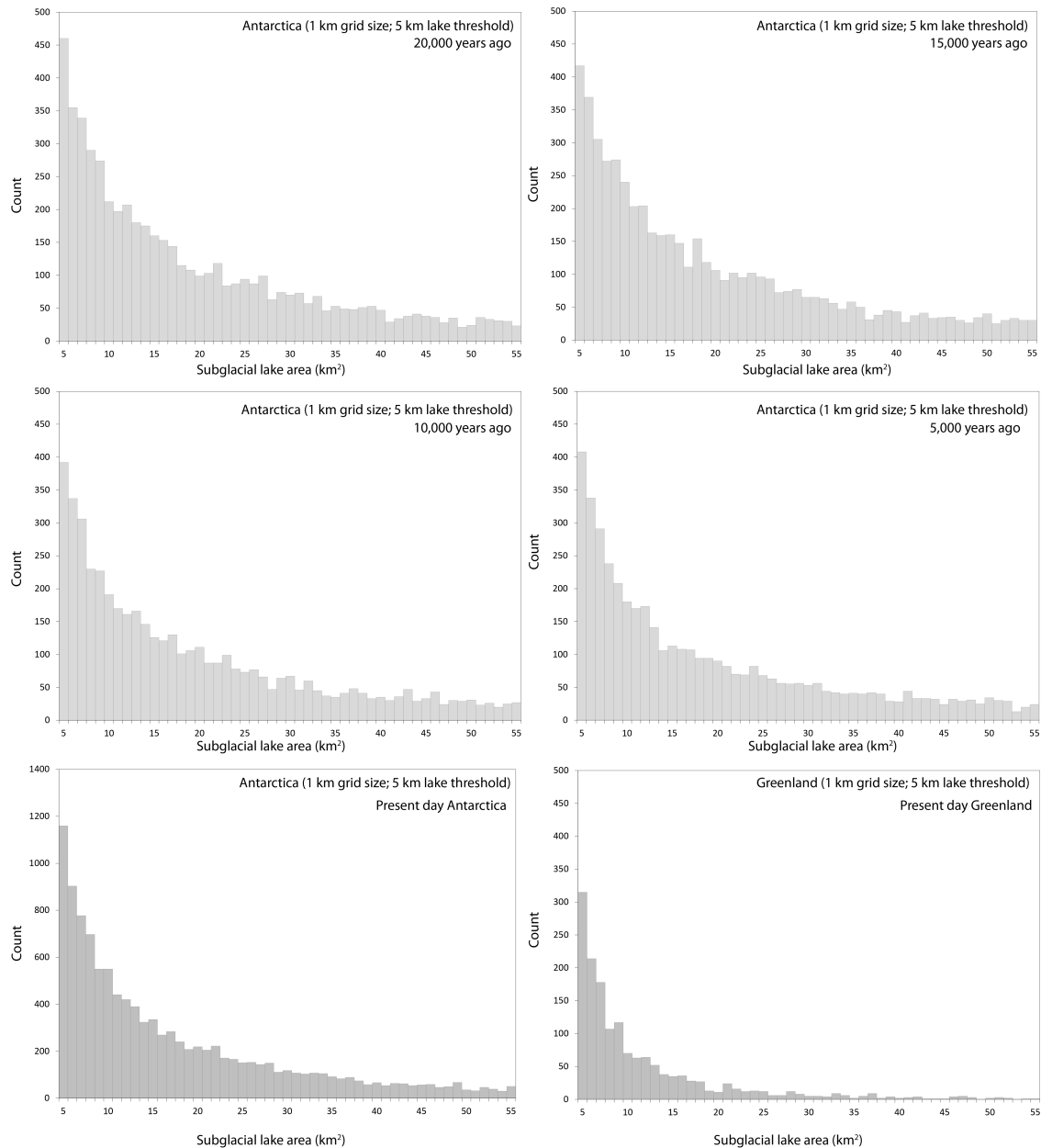


**Fig. 4.** The frequency distribution of potential subglacial lake areas. Bins of  $1 \text{ km}^2$  are used and the maximum area is capped at  $55 \text{ km}^2$ . Larger lakes such as Subglacial Lake Vostok exist, but these would skew the graph adversely and so are left off for simplicity.

#### 4.2 Deglaciation of Greenland Ice Sheet since the Last Glacial Maximum

Like Antarctica, meltwater drainage under the GrIS is predicted to have been broadly stable, with little large-scale re-organisation in hydrology since the LGM (Fig. 6). However, subtle switches in subglacial water drainage are still demonstrated (Fig. 6). For instance, in western Greenland the northern limb of the Jakobshavn drainage network was captured by the Ummannaq system 16 000 yr ago, and the NEGIS drainage catchment expanded southwards during the

10 000 yr time slice (Fig. 6). Also, between 12 and 11 thousand years ago drainage pathways beneath the north GrIS, which previously (and subsequently) were orientated NW and NE, shift to transport water westwards (Fig. 6).

Subglacial lakes are simulated at all time slices through the evolution of the GrIS (Figs. 6, 7, 8). More than 300 subglacial lakes are simulated at each of the time slices between 19 and 16 thousand years ago, with the number then dropping rapidly to  $< 70$  lakes by 9 000 yr before present whereupon it remained relatively steady. Likelihood predictions show a tendency for subglacial lake formation in mountainous ter-

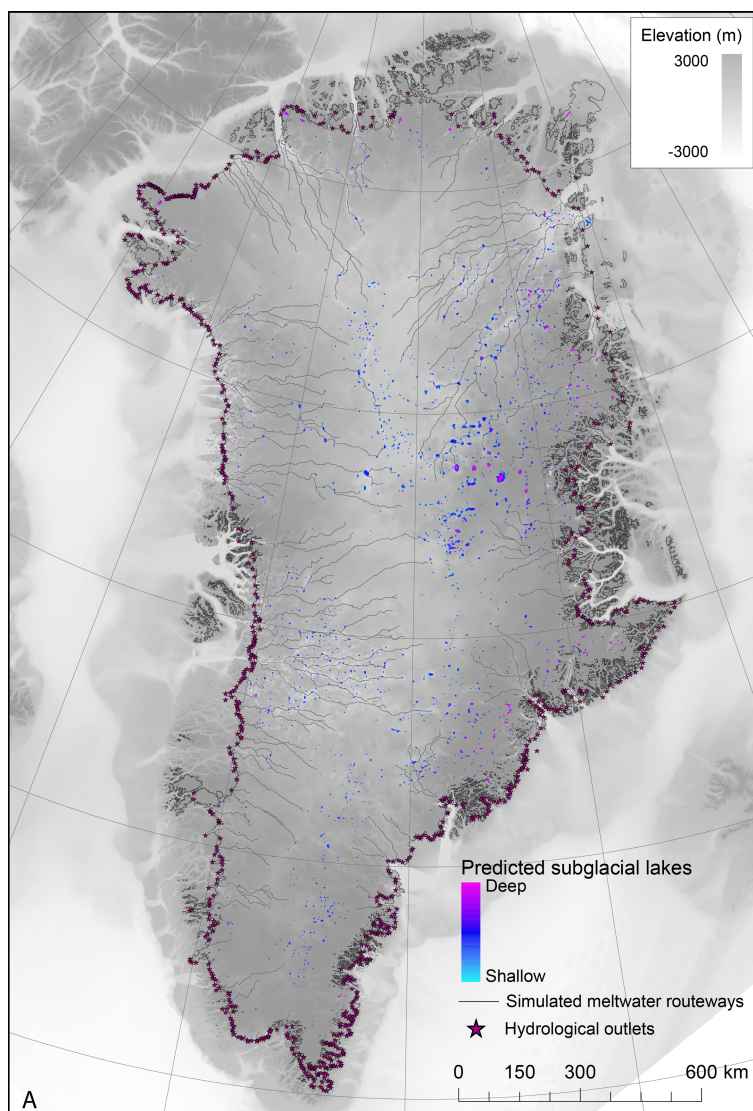


**Fig. 5.** Simulated subglacial drainage pathways and subglacial lakes beneath the GrIS. (A) Illustrates the relationship between ice-sheet topography and observed hydrological outlets (from Lewis and Smith, 2009).

rain, both along the eastern sector of the ice sheet and within fjords (Fig. 7a). Between 19 and 11 thousand years ago > 40% of the simulated lakes are located beyond the present ice-margin position. Lakes are typically small and unstable during the last deglaciation.

Figure 8a demonstrates a decrease in the area covered by subglacial lakes concomitant with a reduction in GrIS size. The period of greatest ice recession, between 14 and 10 thousand years ago, is associated with the largest reduction in subglacial lakes (Fig. 8a). However, the change in subglacial lake area does not decline linearly with ice-sheet size. This is illustrated by the decline in the percentage of the ice-sheet bed occupied by subglacial lakes as the ice sheet waned (Fig. 8b).

## 5 Interpretation and discussion

### 5.1 Antarctica

#### 5.1.1 Recall of known subglacial lakes

Results presented in Sect. 3.1 demonstrate that hydraulic potential calculations are able to successfully recall a large percentage of known subglacial lakes (> 60%) beneath the AIS. The incorporation of the subglacial lake-surface reflector in the bed topography and thickness grids could be considered a fatal flaw in using hydraulic potential equations to identify subglacial lake locations. Yet, the high percentage of subglacial lakes that are recalled questions this logic. For instance, we are able to accurately delimit the extent of Subglacial Lake Vostok (Fig. 1a) despite incorporation of its

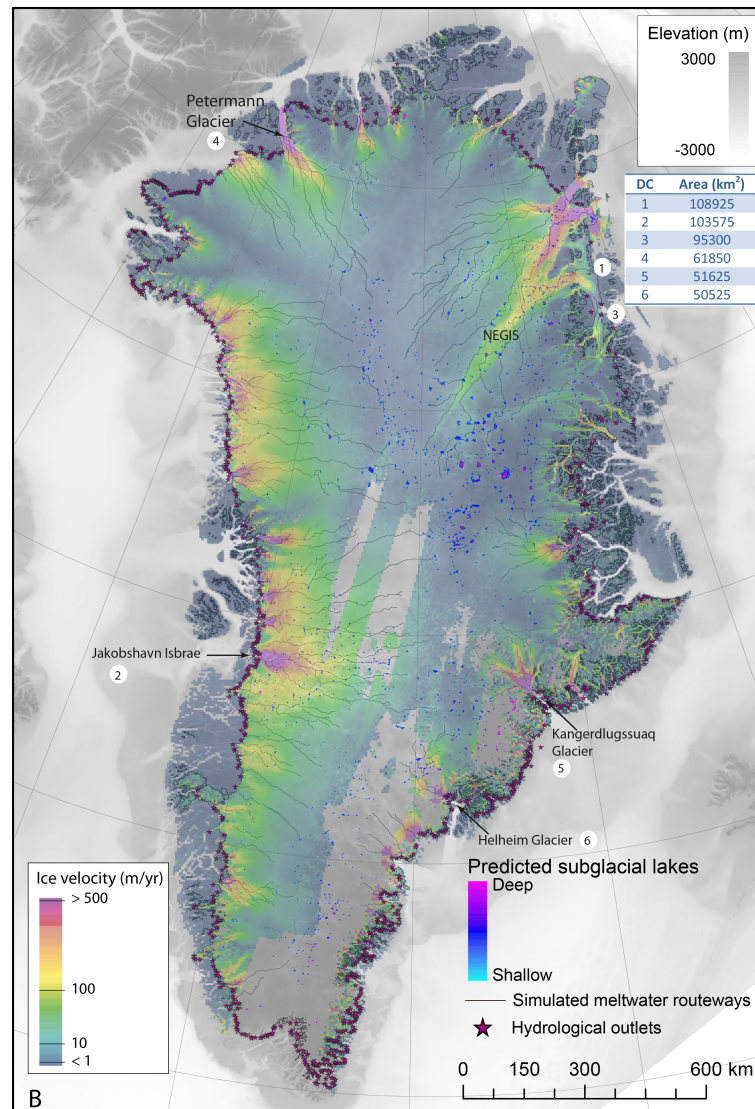


**Fig. 5. (B)** Simulated subglacial drainage pathways and subglacial lakes, and the relationship with ice-surface velocity (Joughin et al., 2010). The six largest drainage catchments (DC) are also listed.

lake-surface reflector into the BEDMAP2 topography grid. We suggest two reasons why this might be the case. Firstly, a subglacial lake would have to be filled to its hydraulic potential surface lip to fully smooth out the minima. While this might be the case for a few subglacial lakes that are just about to drain, the majority are likely to be at some intermediate state of filling (e.g. Smith et al., 2009, and references therein). It is therefore this extra space left to fill up before draining that we are mapping. Secondly, because of the coarse resolution of the grid (1 km or greater) lake outlets may become smoothed, therefore artificially raising the depth required to trigger drainage. Raising the base level at which drainage may occur by smoothing the topography would, however, also pick out basins not able to host subglacial lakes, leading to over-predictions (see Sect. 5.1.2).

Our first-order approximation of potential subglacial lake locations is generally better able to recall known lakes beneath ice streams (Fig. 1). This may be because many ice streams are well surveyed with airborne grids, so the accuracy of the input DEMs is generally higher in these regions. The ability of both smoothed grids to successfully recall known subglacial lakes is significantly enhanced when restricted to just the known lakes  $\geq 5$  km long (Table 1). This seems to confirm the size bias (i.e. that larger lakes are more difficult to remove by smoothing the ice surface), although another reason could be that the large lakes tend to form in deep, tectonically controlled depressions (see Tabacco et al., 2006) and are therefore likely to form irrespective of the ice-surface roughness (Fig. 1b).

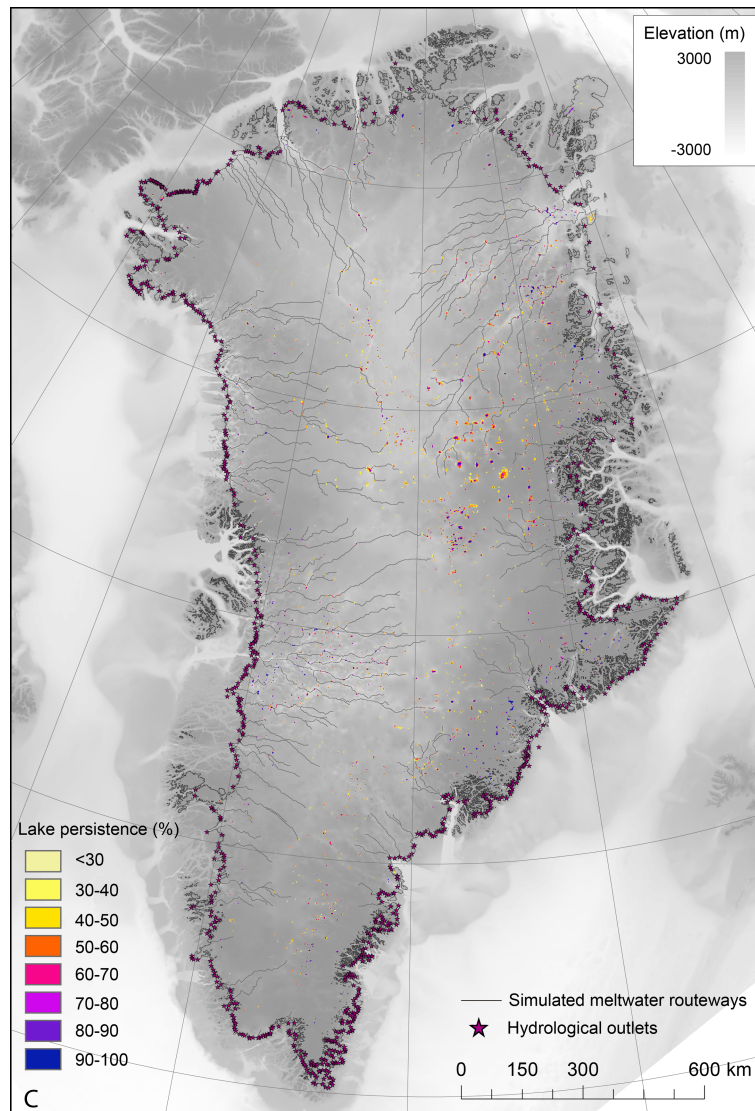


**Fig. 5. (C)** Subglacial lake persistence in response to 50 random bed elevation perturbation experiments, using a normal distribution with a standard deviation equal to the vertical bed uncertainty.

The decline in recall when there is an increase in subglacial lake persistence over a threshold of  $\sim 60\%$  may represent a range of lake sensitivities, and may therefore be a proxy for lake stability. For instance, the deep, tectonically controlled Subglacial Lake Vostok is recalled during every bed elevation perturbation experiment and is therefore likely to be very insensitive to future changes in ice surface or bed slope. Subglacial Lake Vincennes conversely is recalled  $< 80\%$ , which is probably because, despite being wide, it is also formed in a large basin characterised by low relief (Tabacco et al, 2006) and so may be more readily affected by bed or ice-surface elevation changes.

### 5.1.2 Precision of potential subglacial lake locations

The precision of the potential subglacial lake locations is significantly lower ( $< 5\%$ ) than the recall due to the large number of false-negative results. This could be due to (i) error in the input datasets; (ii) many subglacial lakes that remain to be discovered; or (iii) the effect of processes not included in our simple model, e.g. spatial and temporal variations in effective water pressure and ice–hydrology coupling.

Despite our improved knowledge of the topography beneath the AIS, the number of grid cells containing radar data still only comprises 34% of the grounded bed in the updated BEDMAP2 dataset (cf., Fretwell et al., 2013). A large part of the discrepancy between the number of simulated and known subglacial lakes is therefore probably because of

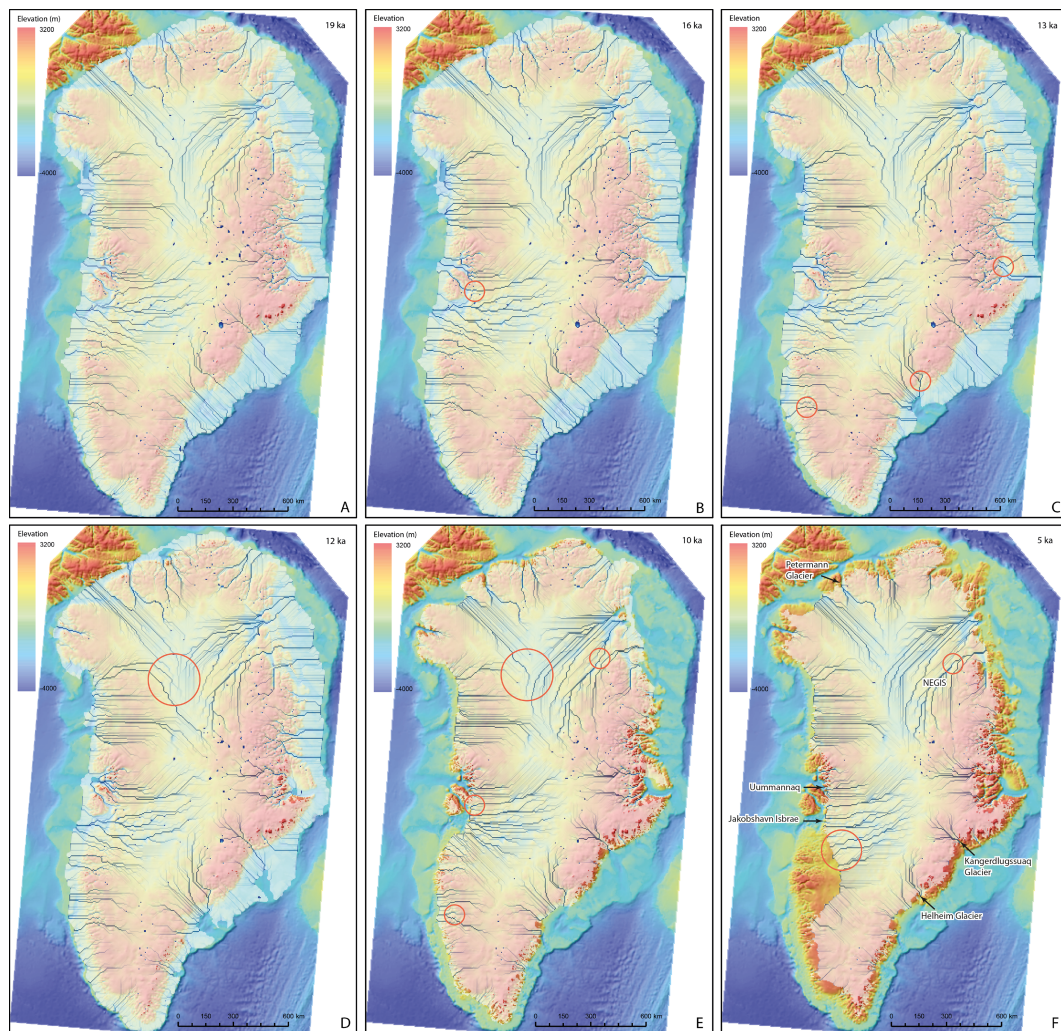


**Fig. 6.** Simulated drainage networks and subglacial lakes for six time slices (A–F) through the evolution of the GrIS since the LGM. Ice surfaces are derived Simpson et al. (from 2009). The opaque white colour delimits the extent of the ice sheet, the blue lines show predicted meltwater pathways and the dark-blue colour shows subglacial lake locations. The red circles highlight drainage switches.

an incomplete knowledge of the bed, and in particular because of erroneous subglacial lakes associated with gridding artefacts (Fig. 1). This is demonstrated by the results of our bed perturbation experiments (Fig. 1c). In regions of the bed characterised by limited or no data (see Fretwell et al., 2013) the majority of lakes occur infrequently ( $< 50\%$ ) when the bed is randomly perturbed. Indeed, removing all simulated subglacial lakes that persist for less than half the perturbation experiments increases the precision to 5% without significantly altering the recall, which implies most of these lakes are artefacts of limited data availability or the interpolation method and can be ignored. Conversely those subglacial lake locations that persist through a large number of random perturbations are insensitive to the bed elevation uncertainty and are therefore more likely to be real.

The large number of potential subglacial lake locations, which persist through a large number ( $> 60\%$ ) of random

perturbations (Figs. 1c, 4), hints at the possibility of many small subglacial lakes yet to be found. However, it is difficult to discriminate between the two remaining error terms without validation of the results against radar data.

### 5.1.3 Potential subglacial lake locations during the deglaciation of the Antarctic Ice Sheet

Our results suggest that subglacial lakes were more prevalent when the ice sheet was larger and extended onto the continental shelf (Fig. 2). This includes repeated palaeo-subglacial lake formation in the rugged interior of Marguerite Bay in isolated basins connected by meltwater channels (e.g. Anderson and Oakes-Fretwell, 2008), and the temporary formation of a shallow subglacial lake in Palmer Deep 15 thousand years ago (see Domack et al., 2006).

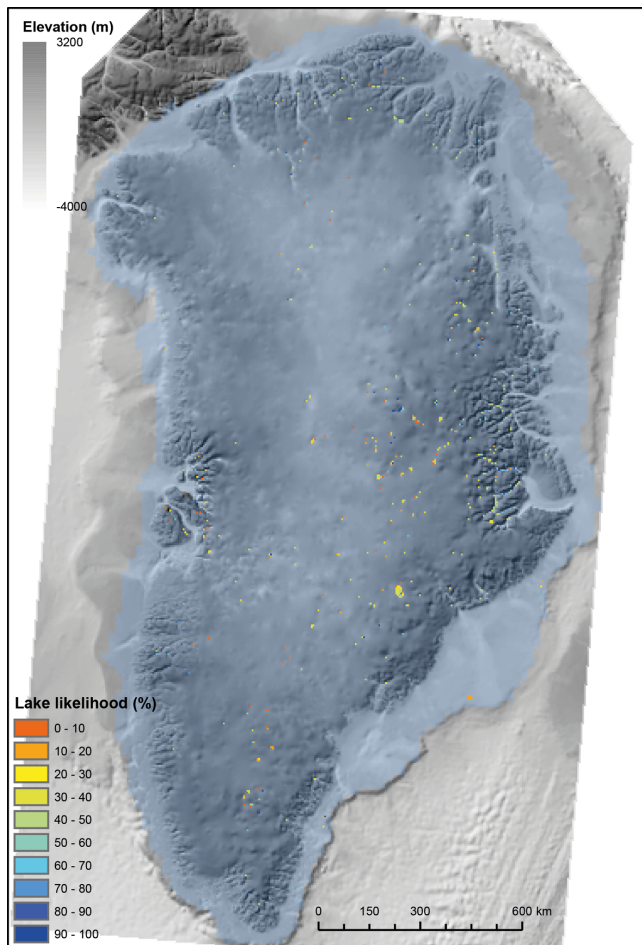


**Fig. 7.** Subglacial lake likelihood map. The likelihood is the percentage time that subglacial lakes occurred in the same location while ice covered that region during deglaciation thus far (not including the present day). Those lakes with a high likelihood are therefore relatively stable.

The ice-surface flattening feedback resulting from subglacial lake formation (e.g. Livingstone et al., 2012, and references therein) sets up the intriguing possibility that many of the present-day subglacial lakes have been inherited from past ice-sheet configurations, and would have already drained without this stabilising feedback. Such an example of hysteresis implies that, for the same geometry, a retreating ice sheet yields considerably more subglacial lakes than one advancing. It therefore follows that many subglacial lakes formed during the last deglaciation, under different ice-sheet geometries, still exist beneath the present-day AIS. The results displayed in Table 2 support this, with 41–44 % of the known subglacial lakes successfully recalled during each deglacial time slice, rising to 50 % when they are all included. Smoothing the ice surface should remove inherited subglacial lakes whose existence depends on the ice-surface flattening feedback. Indeed, there is 25 % less chance

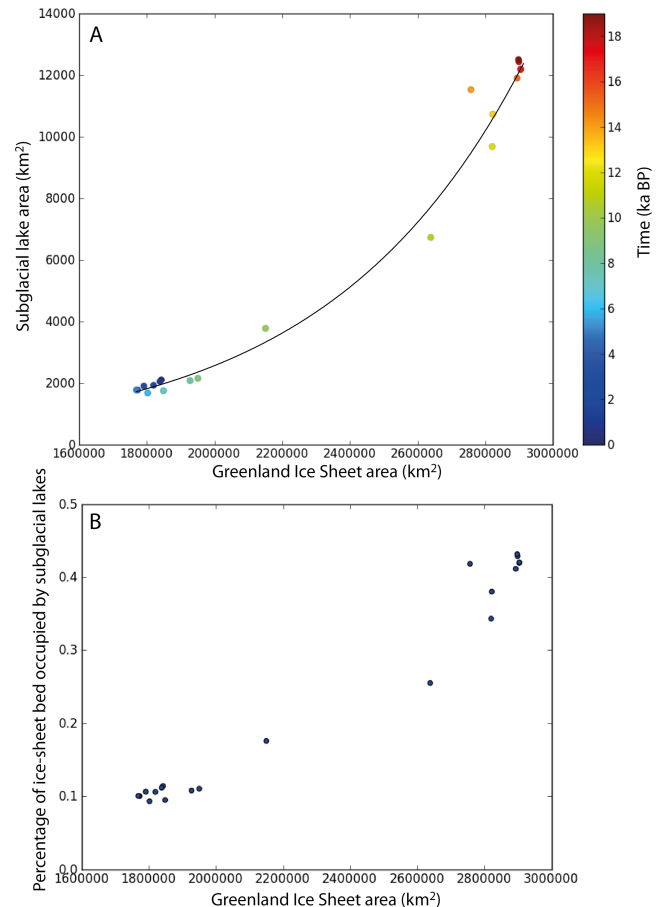


**Fig. 8.** (A) Scatter graph showing the predicted total subglacial lake area vs. the area of the GrIS and colour-coded according to time slice (ka); and (B) the fraction of the grounded ice-sheet bed occupied by subglacial lakes vs. ice-sheet area. The trend line in plot A is an exponential curve that generates an  $R^2$  of 0.99.

of recalling a known subglacial lake when the ice surface has been smoothed and 23 % less chance when using the modelled present-day output (Table 1). We can test whether the subglacial lakes, which have been smoothed out, were derived from past ice-sheet configurations by summing the smoothed subglacial lake simulations with those from the deglacial time slices (see Table 2). The result is a 13 % and 14 % increase in the ability to recall known subglacial lakes using the smoothed and modelled outputs respectively, compared to 8 % when summing the standard experiment with the deglacial time slices (Table 2). This first-order approximation implies that the deglacial simulations can account for  $\sim 13$ –14 % of the known subglacial lakes and that 5–6 % of subglacial lakes persist solely due to the ice-surface flattening feedback.

The implications of this stabilising feedback on short-term subglacial lake stability and longer-term differences between advancing and retreating ice-sheet modes are

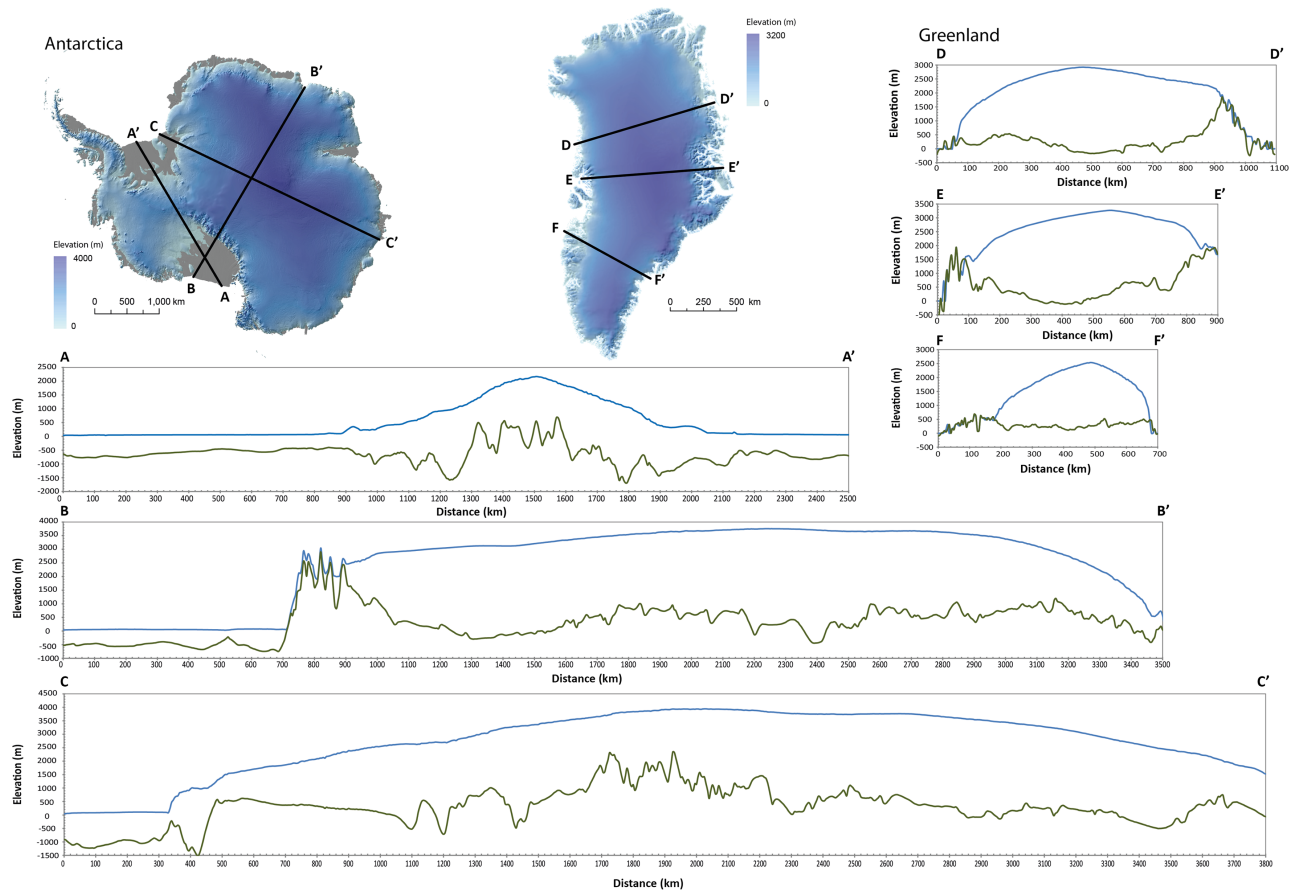


**Fig. 9.** Bed and ice surface profiles for the Greenland and Antarctic ice sheets. Profiles correspond to the inset images of the two ice sheets and both the vertical and horizontal scales are the same for all profiles. Note how the smaller Greenland Ice Sheet has much steeper overall slopes than the Antarctic Ice Sheet, which, because of its size, is characterised by large swathes of relatively flat regions in the interior.

unknown. Certainly, this work suggests that subglacial lakes are more pervasive (and therefore of greater importance) during the deglacial phase, which has resonance for ice-stream formation and flow, bed lubrication, meltwater drainage and eventually ice-sheet collapse.

#### 5.1.4 Meltwater drainage pathways

Our simulated meltwater drainage pathways form a broadly similar network to that calculated by Wright et al. (2008). Variations in drainage patterns between different regions of Antarctica's bed (Fig. 1a) are thought to reflect underlying controls on glacial processes such as slope and structure (cf. Twidale, 2004, and references therein). Classical dendritic patterns are typically associated with very slight surface slopes and/or regions with no significant structural control. It is therefore no surprise that this pattern characterises many of the interior zones of East Antarctica where ice-surface slopes were very low, and regions of the bed smoothed due to lack of data (Fig. 1a). In West Antarctica, especially inland of the Amundsen Sea, and south of the Transantarctic

Mountains, drainage patterns are more angular, possibly due to the basal geology (e.g. the arrangement and spacing of faults and joints). The strongly convergent pattern of meltwater drainage from the South Pole into the Ronne Ice Shelf could reflect the former breaching of a large bedrock ridge, with the subsequent lowering of the drainage level leading to capture of the surrounding hydrology. Finally, strongly parallel drainage geometries imply control of flow by gradient, which is in agreement with the ice-marginal drainage pattern where ice-surface slopes are greatest (Fig. 1a).

Figure 1b illustrates how various subglacial drainage routeways, especially around coastal sectors of the EAIS (e.g. Dronning Maud Land, Terra Adélie and Enderby Land) traverse cold-bedded zones not conducive to meltwater generation or drainage (see Pattyn, 2010). These cold-bedded rims act as seals, promoting subglacial meltwater storage up-glacier, diverting drainage pathways (see Livingstone et al., 2012). However, subglacial water produced upstream of a cold-based region will most likely be frozen on to base of the ice sheet at the thermal boundary between warm-based

**Table 2.** Ice-surface flattening feedback and subglacial lake inheritance: the second to fifth rows illustrate the percentage of known subglacial lakes recalled by each of the modelled deglacial time slices (20, 15, 10 and 5 thousand year intervals). The sixth row is the percentage of known subglacial lakes recalled by the summed deglacial time slices, the seventh row is the percentage recall of the summed deglacial time slices combined with the present-day ice sheet, and the final two rows combine the summed deglacial time slices with the smoothed and modelled present-day ice surfaces respectively. See text for detailed explanation.

Data	Recall (percentage)
Present day (from Table 1)	61
5000 yr ago	41
10 000 yr ago	41
15 000 yr ago	41
20 000 yr ago	44
All deglacial intervals	50
Present day and all deglacial time intervals	69
Smoothed present-day ice surface and all deglacial time intervals	52
Present-day modelled ice surface and all deglacial time intervals	49

and cold-based ice to form the freeze-on plumes observed in radar data (Bell et al., 2011).

Wright et al. (2008) demonstrate that hydrological flow directions can be highly sensitive to slight changes in ice-surface topography. And although the broad-scale pattern of meltwater flow during the last deglaciation is predicted to have been relatively stable (Fig. 2), we also note several regions susceptible to drainage capture or migration, which are moreover shown to be sensitive to perturbations of the present-day ice surface by smoothing. For instance, we observe a similar sensitivity in the drainage of Subglacial Lake Vostok during deglaciation (cf., Wright et al., 2008), while the Siple Coast drainage configuration is shown to have shifted repeatedly during deglaciation using the modelled output (Fig. 3). This is probably due to the low angle of ice slope, which leaves the neighbouring ice-stream drainage networks vulnerable to minor changes in ice thickness. It is perhaps no surprise then that ice-stream stagnation interpreted to indicate meltwater capture has been observed between two of the contemporary ice streams in this region (Anandakrishnan and Alley, 1997). Our analysis suggests this may have been a common occurrence during the last deglaciation, which is in agreement with studies that infer dynamic variability in the behaviour of the Siple Coast ice streams over millennial timescales (Conway et al., 1999; Catania et al., 2012).

## 5.2 Greenland

### 5.2.1 Subglacial lakes beneath the present-day Greenland Ice Sheet

The results for Greenland indicate the potential for subglacial lake formation at the base of the ice sheet, particularly in the rugged eastern sector and beneath major ice streams such as the NEGIS and Jakobshavn Isbrae (Fig. 5). The possibility of subglacial lake formation is further supported by the bed perturbation experiments (Fig. 5c), which indicate persistence of many of the potential subglacial lake locations within the range of bed uncertainty. The analysis therefore implies that, whilst few subglacial lakes have been found beneath the GrIS to date, the ice and bed topographies do permit lake formation (see also Livingstone et al., 2012). We therefore predict that it is only a matter of time before a network of subglacial lakes is identified beneath the GrIS and that our potential subglacial lake locations (both present day and during deglaciation) may provide useful targets for geophysical studies to discover lakes. This is demonstrated by the successful recall of an ice-surface depression anomaly in northern Greenland, inferred to indicate subglacial lake formation, using our subglacial lake predictions (Ekholm et al., 1998).

Apart from the paucity of very large subglacial lakes beneath the GrIS the size, frequency and distribution of lakes are remarkably similar to the AIS (Figs. 1, 4, 5). However, there is a reduced potential for subglacial lake formation beneath the present-day GrIS ( $\sim 1.2\%$  of bed area) compared to the AIS (4%). This leads us to deduce that the bed and ice-surface geometry of the GrIS is less conducive to subglacial lake formation and therefore that subglacial lakes are a less significant component of the hydrological network compared to the AIS. Since the influence of the ice surface on hydraulic potential is about ten times that of the bed (e.g. Shreve, 1972), the lack of subglacial lakes can be reconciled with the steep ice-surface gradients of the GrIS compared to the AIS (see Fig. 9). Thus, the substantially smaller size of the GrIS results in steeper mean surface slopes, thereby precluding an extensive present-day subglacial lake network. This conclusion is supported by Pattyn (2008), who used a full Stokes model to demonstrate the decisive influence of mean-surface slope on subglacial lake stability.

### 5.2.2 Subglacial lake evolution during the deglaciation of the Greenland Ice Sheet

The abundance of subglacial lakes is simulated to decline as the GrIS waned, and as the ice-sheet shrank so too did the propensity for subglacial lake genesis (Fig. 8). This supports our assertion, above, that smaller ice sheets are less conducive to subglacial lake formation because of their steeper mean-surface slopes, while subglacial lake formation is also likely to be favoured when the mountainous rim no longer coincided with the steep ice-sheet margin. The implication

is therefore that the GrIS has lost subglacial lakes through drainage since the LGM (Pattyn (2008); Fig. 9). In addition, Fig. 8b demonstrates how the percentage of the ice-sheet bed occupied by subglacial lakes changed more rapidly (i.e. the gradient was steeper) during the initial stages of deglaciation (19–10 thousand years ago) when the ice sheet was larger (Fig. 8b). This implies that subglacial lakes are more sensitive to changes in ice-sheet size when the ice sheet is larger (i.e. for a given change in ice-sheet area the change in subglacial lake extent is of a higher magnitude).

When the GrIS had expanded onto the continental shelf (19–11 thousand years ago) > 40% of the simulated subglacial lakes lay outside of the present-day ice margin, and would therefore have emerged from under the ice. Other lakes that formed within the bounds of the present-day ice sheet, but are predicted to have drained (Fig. 8) may have survived deglaciation due to the ice-surface flattening feedback (see Sect. 5.1.3).

### 5.2.3 Meltwater drainage routeways

The dendritic pattern of subglacial meltwater flow pathways simulated in this study (Fig. 5) is consistent with the results of Lewis and Smith (2009), and also broadly similar in form to that simulated beneath the AIS. The simulated evolution of the subglacial drainage network since the LGM (Fig. 6) demonstrates the susceptibility of some localities of the ice sheet to subglacial drainage switches, driven by subtle changes in ice surface and bed geometry. Significantly, some of the major present-day ice streams, such as NEGIS and Jakobshavn, display significant changes to their subglacial water flow paths over time (Fig. 6). As for Antarctica, we predict drainage shifts could play a crucial role in controlling ice streaming and behaviour.

## 6 Conclusions

We have demonstrated that the Shreve hydraulic potential equation and simple routing mechanisms in a GIS can be used to successfully recall a high percentage (> 60%) of the known subglacial lakes beneath the AIS. This is despite the surfaces of existing subglacial lakes being used to calculate the bed topography and ice thicknesses used in the calculations. We reason this is because most lakes are not completely full (i.e. at intermediate states of filling) and the relatively coarse grid resolution smooths out the base level at which drainage may occur. In particular, the larger subglacial lakes are easier to recall, although these make up only a small percentage of the total number of lakes.

We simulate significantly more subglacial lakes than those presently identified beneath the AIS, resulting in a low precision. Such a discrepancy is thought to primarily stem from an incomplete knowledge of the bed, as demonstrated by the low frequency of persistent subglacial lakes in regions characterised by large bed elevation uncertainties. And although

our use of a simple hydrological model not coupled to ice dynamics undoubtedly ignores some important mechanisms, we suggest that hundreds if not thousands of subglacial lakes, particularly smaller ones, are yet to be found beneath the AIS. These potential subglacial lake locations provide useful targets for future radar surveys.

By applying the same method to the GrIS we demonstrate the potential for subglacial lake formation at its bed. However, in contrast to Antarctica the subglacial lakes are shown to occupy a smaller fraction of the grounded ice-sheet bed and are characteristically small features. We suggest this is a result of steeper mean surface gradients concomitant with a smaller ice sheet (Figs. 8 and 9). Finally, we demonstrate that many present-day subglacial lakes have been inherited from past ice-sheet configurations due to the subglacial lake ice-surface flattening feedback, and would have already drained without this stabilising effect. The resultant hysteresis, whereby a retreating ice sheet will have many more subglacial lakes than one advancing, has implications for ice-stream formation and flow, bed lubrication and meltwater drainage.

Modelling the present-day drainage networks beneath the Antarctic and Greenland ice sheets has elucidated major meltwater pathways and the form they take. In Antarctica dendritic, angular, convergent and parallel drainage pathways have all been simulated, which have been related to underlying (ice and bed) slope and structural controls. The evolution of the Greenland and Antarctic subglacial drainage networks were assessed by simulating basal meltwater flow at discrete time intervals over the last 21 000 yrs. We reveal key sectors of the two ice sheets that have been vulnerable to past drainage switches. In particular, neighbouring ice-stream drainage networks (e.g. the Siple Coast sector, AIS and the NEGIS, Greenland) with their low-angled slopes are shown to be particularly sensitive to small changes in ice geometry.

Finally, the predictability of subglacial lakes beneath the AIS using hydraulic potential equations and routing techniques suggests this is also a viable methodology for exploring potential palaeo-subglacial lake locations beneath the great Quaternary Northern Hemisphere ice sheets (see Evatt et al., 2006; Livingstone et al., 2013). This approach has the benefit of comprehensive information on the bed properties, but relies on modelled ice-surface topographies.

*Acknowledgements.* This work was supported by a NERC Early Career Research Fellowship awarded to SJL (NE/H015256/1). The data are available upon request from the lead author. We thank Matt Simpson, Pippa Whitehouse and Frank Pattyn for supplying ice-sheet model output on the deglaciation of the Greenland Ice Sheet and Antarctic Ice Sheet, and modelled basal temperature data respectively. The manuscript has benefitted greatly from the comments of two anonymous reviewers and Sasha Carter.

Edited by: R. Bingham

## References

- Anandakrishnan, S. and Alley, R. B.: Stagnation of Ice Stream C, West Antarctica by water piracy, *Geophys. Res. Lett.*, 24, 265–268, 1997.
- Anderson, J. B. and Oakes-Fretwell, L.: Geomorphology of the onset area of a palaeo-ice stream, Marguerite Bay, Antarctic Peninsula, *Earth Surf. Proc. Land.*, 33, 503–512, 2008.
- Bamber J. L., Layberry, R. L., and Gogineni, S. P.: A new ice thickness and bed data set for the Greenland Ice Sheet: 1. Measurement, data reduction, and errors, *J. Geophys. Res.*, 106, 33773–33780, 2001a.
- Bamber J. L., Layberry, R. L., and Gogineni, S. P.: A new ice thickness and bed data set for the Greenland Ice Sheet: 2. Relationship between dynamics and basal topography, *J. Geophys. Res.*, 106, 33781–33788, 2001b.
- Bamber J. L., Griggs, J. A., Hurkmans, R. T. W. L., Dowdeswell, J. A., Gogineni, S. P., Howat, I., Mouginot, J., Paden, J., Palmer, S., Rignot, E., and Steinhage, D.: A new bed elevation dataset for Greenland, *The Cryosphere* 7, 499–510, 2013.
- Bartholomew, I., Nienow, P., Mair, D., Hubbard, A., King, M. A., and Sole, A.: Seasonal evolution of subglacial drainage and acceleration in a Greenland outlet glacier, *Nat. Geosci.*, 3, 408–411, 2010.
- Bell R. E., Ferraccioli, F., Creyts, T.T., Braaten, D., Corr, H., Das, I., Damaske, D., Frearson, N., Jordan, T., Rose, K., Studinger, M. and Wolovick, M.: Widespread persistent thickening of the East Antarctic Ice Sheet by freezing from the base, *Science*, 331, 1592–1595, 2011.
- Catania, G., Hulbe, C., Conway, H., Scambos, T. A. and Raymond, C. F.: Variability in the mass flux of the Ross ice streams, West Antarctica, over the last millennium, *J. Glaciol.*, 58, 741–752, 2012.
- Clarke, G. K. C.: Subglacial processes, *Ann. Rev. Earth Planet. Sci.*, 33, 247–276, 2005.
- Conway, H., Hall, B. L., Denton, G. H., Gades, A. M., and Waddington, E. D.: Past and future grounding-line retreat of the West Antarctic Ice Sheet, *Science*, 286, 280–284, 1999.
- Cuffey, K. M. and Patterson, W. S. B.: *The Physics of Glaciers*, 4th Edn., Elsevier, 2010.
- Dahl-Jensen, D., Gundestrup, N., Gogineni, S. P., and Miller, H.: Basal melt at NorthGRIP modelled from borehole, ice-core and radio-echo sounder observations, *37*, 207–212, 2003.
- Domack, E., Amblás, D., Gilbert, R., Brachfield, S., camerlenghi, A., Rebesco, M., Canals, M., and Uregeles, R.: Subglacial morphology and glacial evolution of the Palmer deep outlet system, Antarctic Peninsula, *Geomorphology*, 75, 125–142, 2006.
- Ekhholm, S., Keller, K., Bamber, J. L. and Gogineni, S. P.: Unusual surface morphology from digital elevation models of the Greenland Ice Sheet, *Geophysical Research Letter*, 25, 3623–2626, 1998.
- Evatt, G. W., Fowler, A. C., Clark, C. D., and Hulton, N. R. J.: Subglacial floods beneath ice sheets, *Philos. T. Roy. Soc. A*, 374, 1769–1794, 2006.
- Fountain, A. G. and Walder, J. S.: Waterflow through temperate glaciers, *Rev. Geophys.*, 36, 299–328, 1998.
- Fretwell, P., Pritchard, H. D., Vaughan, D. G., Bamber, J. L., Barand, N. E., Bell, R., Bianchi, C., Bingham, R. G., Blankenship, D. D., Casassa, G., Catania, G., Callens, D., Conway, H., Cook, A. J., Corr, H. F. J., Damaske, D., Damm, V., Ferraccioli, F., Forsberg, R., Fujita, S., Gim, Y., Gogineni, P., Griggs, J. A., Hindmarsh, R. C. A., Holmlund, P., Holt, J. W., Jacobel, R. W., Jenkins, A., Jokat, W., Jordan, T., King, E. C., Kohler, J., Krabill, W., Riger-Kusk, M., Langley, K. A., Leitchenkov, G., Leuschen, C., Luyendyk, B. P., Matsuoka, K., Mouginot, J., Nitsche, F. O., Nogi, Y., Nost, O. A., Popov, S. V., Rignot, E., Rippon, D. M., Rivera, A., Roberts, J., Ross, N., Siegert, M. J., Smith, A. M., Steinhage, D., Studinger, M., Sun, B., Tinto, B. K., Welch, B. C., Wilson, D., Young, D. A., Xiangbin, C., and Zirizzotti, A.: Bedmap2: improved ice bed, surface and thickness datasets for Antarctica, *The Cryosphere*, 7, 375–393, doi:10.5194/tc-7-375-2013, 2013.
- Fricker, H. A., Scambos, T., Bindschadler, R., and Padman, L.: An active subglacial water system in West Antarctica mapped from space, *Science*, 315, 1544–1548, 2007.
- Fricker, H. A., Scambos, T., Carter, S., Davis, C., Haran, T. and Joughin, I.: Synthesizing multiple remote-sensing techniques for subglacial hydrologic mapping: application to a lake system beneath MacAyeal Ice Stream, West Antarctica, *J. Glaciol.*, 56, 187–199, 2010.
- Hallet, B.: Subglacial regelation water film, *J. Glaciol.*, 17, 209–221, 1979.
- Hubbard, B., Sharp, M. J., Willis, I. C., Neilsen, M. K., and Smart, C. C.: Borehole water-level variations and the structure of the subglacial hydrological system of Haut Glacier d’Arolla, Valais, Switzerland, *J. Glaciol.*, 41, 572–583, 1995.
- Joughin, I., Smith, B. E., Howat, I. M., Scambos, T., and Moon, T.: Greenland flow variability from ice-sheet wide velocity mapping, *J. Glaciol.*, 56, 415–430, 2010.
- Kamb, B.: Glacier surge mechanism based on linked cavity configuration of the basal water conduit system, *J. Geophys. Res.*, 96, 585–595, 1987.
- Kamb, B.: Basal zone of the West Antarctic ice streams and its role in lubrication of their rapid motion, in: *The West Antarctic Ice Sheet: behaviour and environment*, edited by: Alley, R. B. and Bindschadler, R. A., Antarctic Research Series, 77, Washington DC, American Geophysical Union, 157–199, 2001.
- Kingslake, J. and Ng, F.: Modelling the coupling of flood discharge with glacier flow during jökulhlaups, *Annals of Glaciology*, 54, 25–31, 2013.
- Lappégard, G., Kohler, J., Jackson, M., and Hagen, J. O.: Characteristics of subglacial drainage systems deduced from load-cell measurements, *J. Glaciol.*, 52, 137–148, 2006.
- Lewis, S. M. and Smith, L. C.: Hydrological drainage of the Greenland Ice Sheet, *Hydrol. Process.*, 23, 2004–2011, 2009.
- Livingstone, S. J., Clark, C. D., Piotrowski, J. A., Tranter, M. J., Bentley, M. J., Hodson, A., Swift, D. A., and Woodward, J.: Theoretical framework and diagnostic criteria for the identification of palaeo-subglacial lakes, *Quaternary Sci. Rev.*, 55, 88–110, 2012.
- Livingstone, S. J., Clark, C. D., and Tarasov, L.: Modelling North American palaeo-subglacial lakes and their meltwater drainage pathways, *Earth Planet. Sci. Lett.*, 375, 13–33, 2013.
- Lliboutry, L.: Local friction laws for glaciers: a critical review and new openings, *J. Glaciol.*, 23, 67–95, 1979.
- Nienow, P. W., Sharp, M., and Willis, I.: Seasonal changes in the morphology of the subglacial drainage system, Haut Glacier d’Arolla, Switzerland, *Earth Surf. Proc. Land.*, 23, 825–843, 1998.

- Oswald, G. K. A. and Gogineni, S. P.: Recovery of subglacial water extent from Greenland radar survey data, *J. Glaciol.*, 54, 94–106, 2008.
- Oswald, G. K. A. and Gogineni, S. P.: Mapping basal melt under the Northern Greenland Ice Sheet, *IEEE T. Geosci. Remote*, 50, 585–592, 2012.
- Pattyn, F.: Investigating the stability of subglacial lakes with a full Stokes ice-sheet model, *J. Glaciol.*, 54, 353–361, 2008.
- Pattyn, F.: Antarctic subglacial conditions inferred from a hybrid ice sheet/ice stream model, *Earth Planet. Sci. Lett.*, 295, 451–561, 2010.
- Robin, G. de Q., Swithinbank, C. W. M., and Smith, B. M. E.: Radio Echo Exploration of the Antarctic Ice Sheet, International symposium on Antarctic glaciological exploration (ISAGE), Hannover, New Hampshire, USA, 3–7 September 1968, 1970.
- Röthlisberger, H.: Water pressure in intra- and subglacial channels, *J. Glaciol.*, 11, 177–203, 1972.
- Rutt, I. C., Hagdorn, M., Hulton, N. R. J. and Payne, A. J.: The Glimmer community ice sheet model, *J. Geophys. Res.*, 114, F02004, doi:10.1029/2008JF001015, 2009.
- Schoof, C.: Ice-sheet acceleration driven by melt supply variability, *Nature*, 468, 803–806, 2010.
- Sergienko, O. V. and Hulbe, C. L.: 'Sticky spots' and subglacial lakes under ice streams of the Siple Coast, Antarctica, *Annals of Glaciology*, 52, 18–22, 2011.
- Sharp, M., Gemmell, J. C., Tison, J.-L.: Structure and stability of the former subglacial drainage system of the Glacier de Tsanfleuron, Switzerland, *Earth Surf, Proc. Land.*, 14, 119–134, 1989.
- Shreve, R. L.: Movement of water in glaciers, *J. Glaciol.*, 11, 205–214, 1972.
- Siegert, M. J., Le Brocq, A., and Payne, A. J.: Hydrological connections between Antarctic subglacial lakes, the flow of water beneath the East Antarctic Ice Sheet and implications for sedimentary processes, in: *Glacial Sedimentary Processes and Products*, edited by: Hambrey, M. J., Christoffersen, P., Glasser, N. F., and Hubbard, B., Special Publication 39 of the IAS, Wiley-Blackwell, 2007.
- Simpson, M. J. R., Milne, G. A., Huybrechts, P., and Long, A. J.: Calibrating a glaciological model of the Greenland Ice Sheet from the Last Glacial Maximum to present-day using field observations of relative sea level and ice extent, *Quaternary Sci. Rev.*, 28, 1631–1657, 2009.
- Smith, B. E., Fricker, H. A., Joughin, I. R., and Tulaczyk, S.: An inventory of active subglacial lakes in Antarctica detected by ICE-Sat (2003–2008), *J. Glaciol.*, 55, 573–595, 2009.
- Tabacco, I. E., Cianfarra, P., Forieri, A., Salvini, F. and Zirizzotti, A.: Physiography and tectonic setting of the subglacial lake district between Vostok and Belgica subglacial highlands (Antarctica), *Geophysical Journal International*, 165, 1029–1040, 2006.
- Twidale, C. R.: River patterns and their meaning, *Earth Sci. Rev.*, 67, 159–218, 2004.
- Walder, J. S. and Hallet, B.: Geometry of former subglacial water channels and cavities, *J. Glaciol.*, 23, 335–346, 1979.
- Whitehouse, P. L., Bentley, M. J., and Le Brocq, A. M.: A deglacial model for Antarctica: geological constraints and glaciological modelling as a basis for a new model of Antarctic glacial isostatic adjustment, *Quaternary Sci. Rev.*, 32, 1–24, 2012.
- Wingham, D. J., Siegert, M. J., Shepherd, A., and Muir, S.: Rapid discharge connects Antarctic subglacial lakes, *Nature*, 440, 1033–1036.
- Wright A. P. and Siegert M. J.: A fourth inventory of Antarctic subglacial lakes, *Antarctic Science*, 24, 659–664.
- Wright, A. P., Siegert, M. J., Le Brocq, A. M., and Gore, D. B.: High sensitivity of subglacial hydrological pathways in Antarctica to small ice-sheet changes, *Geophys. Res. Lett.*, 45, L17504, doi:10.1029/2008GL034937, 2008.